An Automatic Instrument for the Determination of Astro-Azimuth

JOSEPH E. CARROLL*
Control Data Corporation, Minneapolis, Minn.

Evaluation of future inertial equipment will require test pad azimuth much more frequently than is possible with existing theodolites. The present paper proposes a completely automatic instrument for impersonal astronomic observations, which can monitor azimuth motion over periods as short as a few minutes. The instrument is composed of a wide-angle optical system, vertically oriented and rigidly attached to the Earth, which scans the night time star field by virtue of the Earth's rotation. A fixed multislit reticle positioned at the focal surface interrupts the star image illumination to produce electrical pulses from a photodetector. These pulses are timed and processed by a central computer which performs the tasks of star/slit identification and position and azimuth computation. An analysis is presented of the application of such an instrument to the rapid determination of precise azimuths for a permanent test pad facility. Instrument design and data processing concepts are described. Simulation data are presented in the areas of star availability (data rate) and error analysis.

Introduction

THE determination and monitoring of north azimuth is frequently required for inertial component testing in specially built facilities. As such, the increasing accuracy of inertial sensors during the coming decade will stretch current azimuth determination techniques beyond their point of practicality. Indeed, in a few cases, this has already occurred, since some sensors (such as the advanced ESG free rotor) are capable of operation in the sub-arcsec region.

Although azimuth determinations to a fraction of an arcsec are possible with present theodolite methods,[1] they impose requirements in terms of operator skill and observation time that make them impractical for a continuing program (e.g., every clear night and all night long). In addition, the several hours of sightings necessary to achieve reliable azimuth can subject the result to systematic errors if azimuth shifts occur during this time, which are by no means unlikely.

To answer the question "How much time can one allow for the measurement of azimuth?", we note that in one instance, a slab rotation of 22 arcsec in 3 hr was observed.[8] This is extremely rare, however. Most peak motions do not exceed 0.25 arcsec/hr.† To observe these and slower rates, a 30-min observation time should be considered as an upper limit unless azimuth drift is incorporated in the mathematical model.

We propose a fundamentally different approach that is impersonal in both measurement and data reduction and is therefore inherently free from human mistakes and body heat distortions. The sensing instrument is simple and has no moving parts. This will significantly enhance calibration stability and should lead to very repeatable results. The time required to obtain a "fix" is usually in the range of 10–20 min, depending upon the zenith sky star density. This is sufficiently short that rate terms in position (level) and azimuth are not required in the mathematical model. However, no instrument change is needed should it later prove useful to expand this model.

The permanent installation of such an instrument requires (besides the usual weather enclosures and stable pier) that the astronomic position of the site be surveyed to within 0.28 arcsec in longitude but only 2.3 arcmin in latitude (Appendix). This task, which need only be accomplished once, permits significant simplification of the instrument and data processing over what would be required should position be unknown.

Basically, the concept relies on timing the transits of star images as they cross a fixed slit pattern as illustrated in Fig. 1. Such photoelectric registration of star transits dates from the 20's. The first successful use of these transits was made in Russia in a series of clock-correction experiments from 1937 to 1941.[2] Not until the 60's, however, were such detections applied to geodetic astronomy.[3,4] Currently, the Air Force Cambridge Research Laboratory (AFCRL) is modifying a T4 theodolite for such work.[5]

A previous paper by the author[6] presented many of the concepts and analyses employed in the current instrument but concentrated on the determination of astronomic position in field situations. Only slight mention was made of azimuth. The current paper extends the design to incorporate azimuth readout and also presents new material in the areas of star availability, error analysis, and instrument design.

System Configuration

The heart of the new proposed scheme for determining and monitoring azimuth is composed (see Fig. 1) of a wide-angle optical system with a radial pattern of slits located at its focal surface and a photodetector located behind these slits. If such a system is rigidly fastened to the Earth and is directed overhead, the pattern of zenith stars will move across the slit reticle creating pulses at the photodetector output. These pulses each represent the transit of one star across one slit and can be timed (by WWV, call letters of the National Bureau of Standards, for example). The transit time patterns thus generated are fed directly into a computer or recorded for later processing. In any event, an appropriate computer program can identify the transits and determine from them the celestial pointing direction and north azimuth of the sensor.

To make use of this information in determining the north azimuth of a test pad reference mirror, the star sensor should be located (see Fig. 2) sufficiently far from the main building to afford an unobstructed view of the zenith sky (including the avoidance of atmospheric disturbances caused by building

Received August 13, 1969; presented as Paper 69-861 at the AIAA Guidance, Control, and Flight Mechanics Conference, Princeton, N.J., August 18–20, 1969; revision received June 8, 1970.

* Staff Specialist, Edina Space and Defense Systems.

† Based on a dirunal sinuoisdal motion of 2 arcsec peak-to-peak.

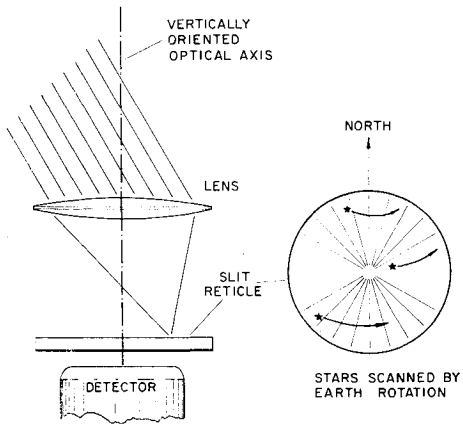

Fig. 1 Schematic component arrangement for photoelectric star detection.

temperature) and at an elevation so as to permit approximately horizontal azimuth transfer. (See Appendix).

For the basement facility shown, the star sensor resides in a well of its own, having a removable cover just above ground level. A plane-parallel plate of glass provides a quite stable atmosphere near the aperture as well as protecting the sensor from dust and debris. The sensor well is connected to the main test room via a walkway for maintenance and an evacuated port (or one filled with neon) for azimuth transfer. Actual azimuth transfer is accomplished using theodolite sightings on both the star sensor azimuth mirror and the facility reference mirror, the results being corrected by the computer output. An alternative method would employ an automatic autocollimator switched periodically from the star sensor mirror to the facility mirror (e.g., via a pentaprism swung into place). This fully automatic approach can be generalized to have the star sensor mirror normal pass by a number of inertial test stands into an autocollimator. A series of pentaprisms (one for each test stand) could then be sequentially switched into the beam. Either arrangement, with all information fed to a central computer, would provide nearly continuous and automatic monitoring of north azimuth.

Simplification of instrument design requires that the astronomic position of the star sensor be known to permit correction of the computed azimuth (see Appendix). If position were not known, the star sensor would have to contain a reversal bearing and level sensor such as is proposed in Ref. 6. Because of the permanency of the sight, a significant degree of instrument simplification can thus be effected.

The principal advantages of such a method for automatic and precision azimuth determination are tabulated in Table 1.

Table 1 Advantages of the new method

Features	Advantages
Automatic operation	No precision manual measurements required (except for azimuth transfer). Elimination of personal equation and mistakes.
Instrument isolation	Environment can be tailored to instrument rather than operator. Elimination of operator as source of heat.
Rapid data accumulation	Rapid tracking of test pad azimuth variations. Quick recovery after occasional cloud cover.
Zenith sky	Minimizes refraction effects.
Radial slit pattern	Focal length not required to be known or remain constant. No need to correct for vertical refraction. Effects of optical aberrations minimized.
Insensitivity to level variations	No requirement for level control, stability or precise knowledge (see Appendix).

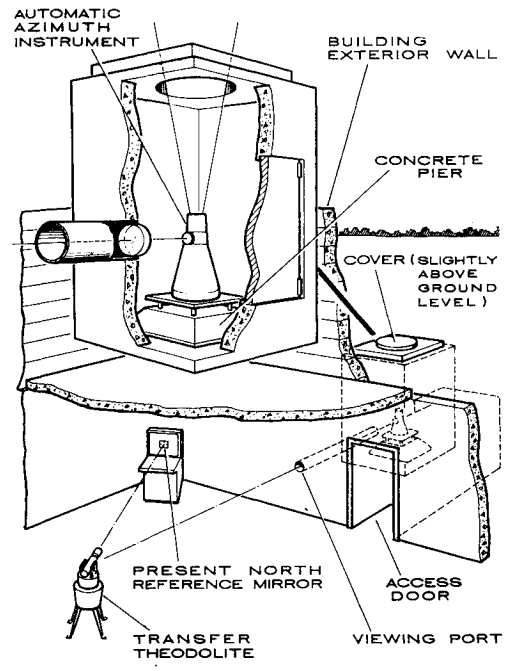

Fig. 2 Exterior sensor location facilitates zenith operation as well as transfer into the test room.

A typical operational sequence might proceed as follows: at sundown, the hatch is opened, the sensor approximately leveled, and the computer/electronics system checked out. When sufficiently dark, the system is turned on and begins to accumulate transits. Depending upon star pattern density, a complete determination can be made in a few minutes. Each transit thereafter serves to increase accuracy, until the point is reached at which the oldest transits are deleted from the solution (depending upon the length of time over which the math model is valid and the desired accuracy). For the rest of the night (unless observing is interrupted) the solution is based upon only the latest transits (e.g., over the last 15 min) and a continuous azimuth value is printed out.‡ At the approach of dawn, the system can be shut down in the reverse order of its set-up.

Instrument Design

The star sensor (Fig. 3) is of simple design, having no moving parts except for the coarse level adjustment screws. The optical design is somewhat unconventional in order to assure high quality images over a wide field of view. As discussed later, the tradeoff between field of view, number of slits, and limiting detectable star magnitude is not clear-cut. The design shown in Fig. 3 possesses a 16° field of view, has 13 slits/fan in the reticle, and detects stars down to 5.6 magnitude. All surfaces (including the focal surface) are spherical and concentric to the aperture, except that the interface between the two types of glass in the meniscus corrector (which is spherical) is not concentric with the other surfaces. The primary mirror suffers from spherical aberration which is removed at one wavelength by the corrector. This refractive element introduces chromatic aberration, which is minimized by the use of glasses of differing index of refraction separated by a nonconcentric interface. Optimization of the optical design requires careful consideration of the response of the photodetector, choice of glasses, and many computer ray-trace runs.

Two potentially serious problems arise from a) defocusing of the image caused by a change in the primary mirror-focal surface distance (the back focus), and b) tilting of the instru-

‡ Or used to correct some other automatic device.

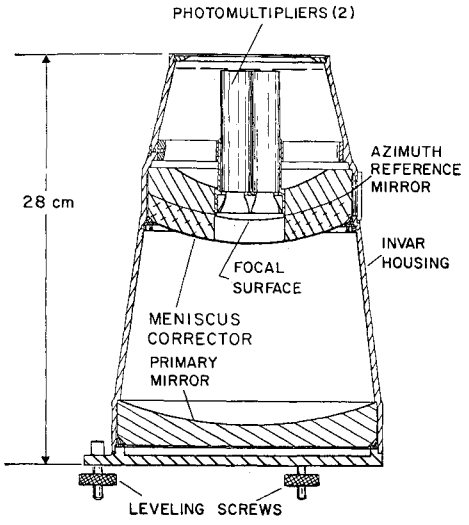

Fig. 3 Simple sensor construction promises ultimate accuracy and stability.

ment axis caused by thermal gradients. In the present application, little chance will exist for a thermal gradient to appear, since the instrument remains undisturbed in its well except for the slow effects due to external conditions. Furthermore, if the gradient were permanent (not a likely event), and the tilt did not exceed a few minutes of arc, no azimuth error would result (see Appendix). It is important, however, that the temperature gradient environment, if present, remain stable.

The design shown in Fig. 3 employs Invar (coefficient of expansion 0.9×10^{-6}/°C) for the housing. Ultra-low-expansion ($0 \pm 0.03 \times 10^{-6}$/°C) glass is used for the mirror, but the glasses used for the meniscus corrector have an average expansion of 8.0×10^{-6}/°C. The focal surface is attached to the meniscus corrector, and the latter makes contact with the housing at its upper surface. As temperature increases, therefore, the housing expands, pulling the corrector away from the primary mirror, but the corrector itself expands, pushing the focal surface towards the mirror. These two motions can be made to cancel exactly, as shown in Fig. 4, if the distance between the glass lands L and the distance between the focal surface and the corrector land l are in a ratio inverse to that of the coefficients of expansion of Invar and glass. Such cancellation is necessary to maintain the back focus (BFL) constant. That the scheme works has been demonstrated in a recent program where an optical system designed as above (smaller field

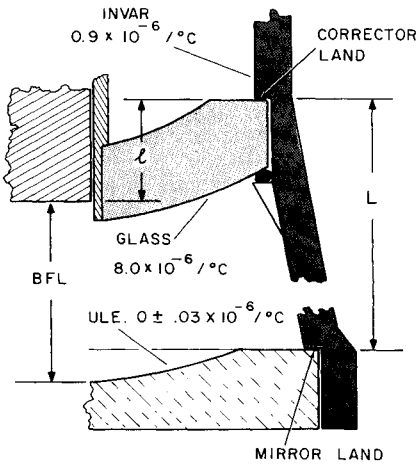

Fig. 4 Layout of star sensor mounting surfaces maintains back focal length (BFL) constant over a wide temperature range if $l/L = (0.9 \times 10^{-6}/8.0 \times 10^{-6})$. (Housing material must have expansion coefficient smaller than that for the corrector.)

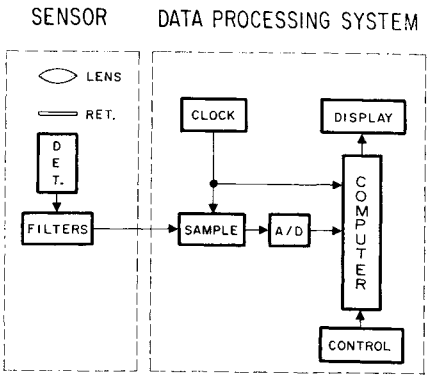

Fig. 5 System block diagram shows real-time azimuth computation capability.

of view) was focused at a laboratory ambient of 25°C and was then taken outside into −26°C for tests with real stars. No refocusing was necessary, and no image degradation was noticed.

The focal surface is a sphere of 4-in. radius. Each slit is 5-μm wide (10 sec of arc) by 1.4-cm long (8°). The slits are arranged as shown in Fig. 1 into two fans (one north, the other south) of 13 slits each. Starlight focused on these slits passes through and is collected onto the cathode of a photomultiplier tube—one tube for each fan of slits. These tubes are of the miniature type, e.g., EMR Model 531N-01-14.

The block diagram in Fig. 5 shows the recommended signal processing technique. The photomultiplier output pulse is ~1-sec wide. This pulse is sampled and digitized ten times/sec for presentation to the computer. These samples are then fitted in the computer, and the peak time is taken from the fit. (The details of this are presented more fully in Ref. 6.) A local clock synchronized with WWV provides the time base.

Star Availability

In Ref. 6, the tradeoff between number of star transits in a given interval, field of view, number of slits per fan, and limiting detectable star magnitude was analytically based on an assumed uniform star distribution. Recently, more exact work has been possible using the actual star distribution from the SAO catalog.[7] A computer program scanned the slit reticle through the celestial sphere counting the star transits of various magnitudes. The program reviewed only the sky overhead at 45° north latitude and started at 100 locations positioned uniformly around the pole. Representative results are shown in Figs. 6–8. (In this section, 20 transits has been chosen as a desirable number, based on the results presented in Fig. 9.)

Figure 6 shows that the time required to accumulate 20 transits is inversely proportional to the number of slits in the

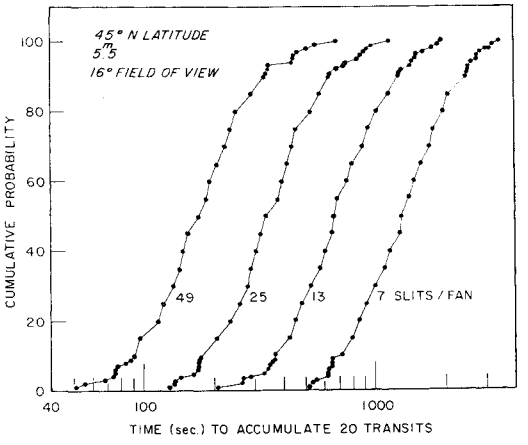

Fig. 6 Cumulative probability of acquiring 20 transits for a randomly directed sensor.

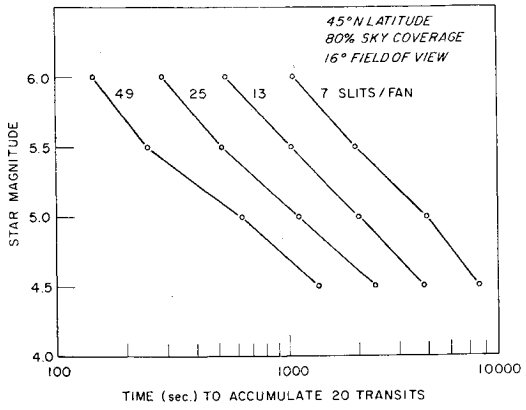

Fig. 7 Dependence of star detection requirements on allowable measurement time and number of slits.

reticle. Figure 7 shows that doubling the number of slits is almost equivalent to decreasing the limiting detectable magnitude by 0.5. The 80% sky coverage was chosen somewhat arbitrarily as indicating wide applicability while not requiring excessive time to reach the remaining portions.§ Figure 8, compiled from Fig. 7 and its counterparts for the other fields of view examined, shows that a 4° increase in the field of view is approximately equivalent to a star magnitude decrease of about 0.25.

The design chosen in Fig. 3 (16° field of view, 5.6 limiting star magnitude, 13 slits/fan, and 80% coverage in excess of 20 transits in 15 min) represents the compromise between a) trying to minimize the fabrication problem by keeping down the field of view, number of slits, and star magnitude¶ and b) trying to accumulate enough star transits in as short a time as possible. Another tradeoff parameter is working here too; pulse overlap or contamination due to slightly dimmer stars. Approximate analysis shows that, for transits accumulated in 15 min, for the present design, about 20% of the desirable transits will be contaminated by stars which are 2.5 magnitudes dimmer than the limiting magnitude (about 10% intensity). If the 20 transits were accumulated in 7 min, 40% would be contaminated; if accumulated in 30 min, only 10%. In dense regions of the sky it will be operationally advisable to raise the threshold to maintain the detection rate at 20/15 min.

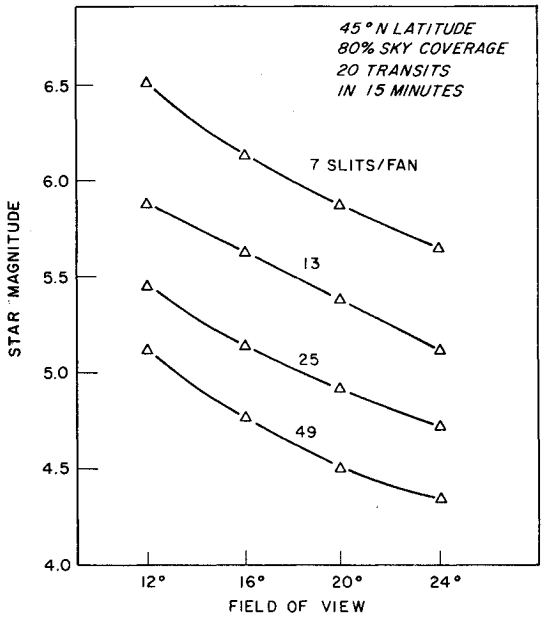

Fig. 8 System tradeoffs between star detection, reticle complexity, and optical field of view.

§ Almost half of the sky is scanned during any one night.

¶ This influences aperture size via signal-to-noise considerations.[6]

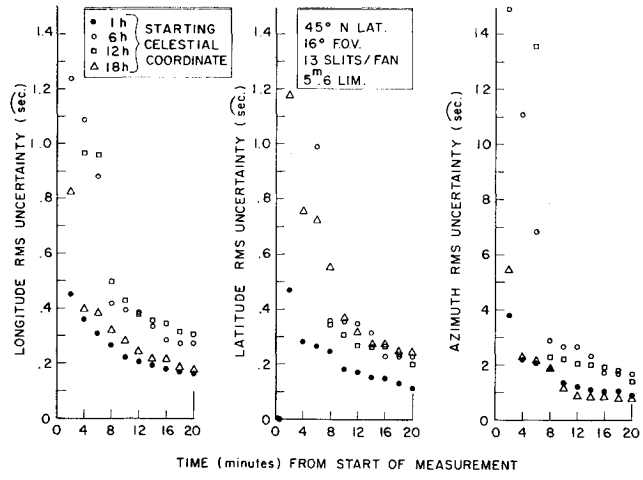

Fig. 9 Position and azimuth RMS uncertainties as a function of measurement time for four positions around the celestial sphere.

Error Analysis

Each star transit pulse is about 1 sec of time wide. Extensive analysis and measurement experience indicate that the determination of the center of this pulse can be accomplished to about a factor of 8 for limiting magnitude stars. Since, for photomultiplier tubes, the noise is dominated by that in the signal itself (random arrival of photons), transit pulses for stars brighter than the limiting value can be interpolated by a factor greater than eight by the square root of the ratio of intensities I

$$8[I(\text{mag} = m)/I(\text{mag} = 5.6)]^{1/2} = 8 \times 10^{-0.2(m-5.6)}$$

so that for a star of magnitude $m = 5$, the interpolation factor is 10.6, for $m = 4$, it becomes 16.7, and so forth.

These individual transit time errors can be combined through the real star and slit geometry in an error analysis program, the results of which are shown in Figs. 9 and 10. The slit pattern is scanned through the star catalog starting at four right ascension values (to obtain a representative sample around the sky). From the individual transit errors are computed the position and azimuth one-sigma uncertainties.

The factor of 10 relation between azimuth and position uncertainties is just the sine of the mean off-axis angle: sin

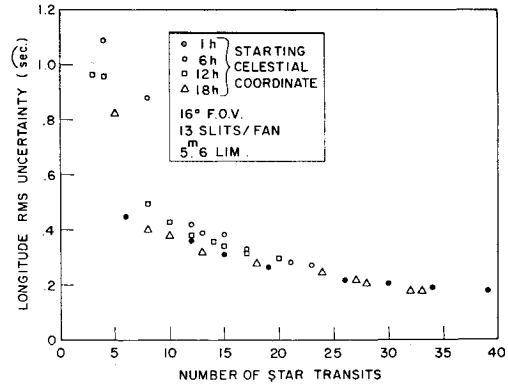

Fig. 10 Demonstration that RMS uncertainty depends strongly on total number of star transits.

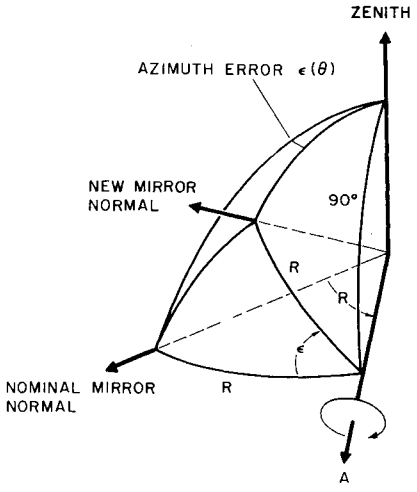

Fig. 11 Movement of mirror normal for nominally horizontal azimuth transfer.

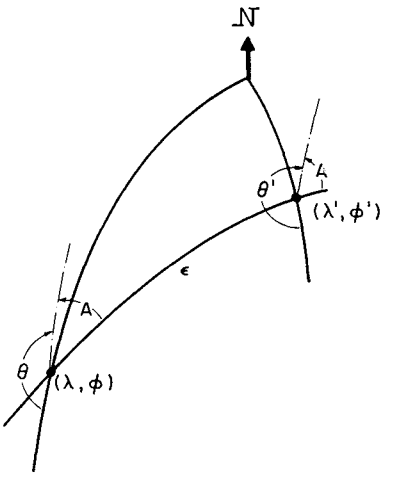

Fig. 13 Demonstration that azimuth depends upon assumed position.

$(8°/2^{1/2})$ = sin 5.66° = 0.099. This shows the dependence of azimuth accuracy on field of view. The accuracy of azimuth will always be less than that for position, however, since to be equal would require a 180° field of view, clearly not very practical in the present application.

The data of Fig. 9 are replotted in Fig. 10 using number of transits rather than time as abscissa. Only the longitude component is shown, but comparison of the two figures clearly indicates that accuracy depends more strongly on the number of transits than on star density. Stated in another way, by the time 20 transits have been accumulated, the transit geometry has become quite uniform, independent of sky quadrant scanned.

Summary

An alternative approach has been presented to the current theodolite method of determining the north azimuth of a reference mirror. It incorporates photoelectric detection of star transits past slits in a reticle located at the focal surface of a wide-angle optical system oriented in the vertical. Analysis shows that a determination can be accomplished in about 15 min with 16°-field-of-view optics using stars down to 5.6 magnitude. This results in a practical optical design and photomultiplier tube detector. The proposed concept represents a fundamental break with past methods and thereby opens up a potential for application to other areas besides the monitoring of test pad azimuths. Some of these are: astronomical surveying, star catalog generation, atmospheric studies, measurement of polar motion, and motion dynamics of extra-terrestrial bodies.

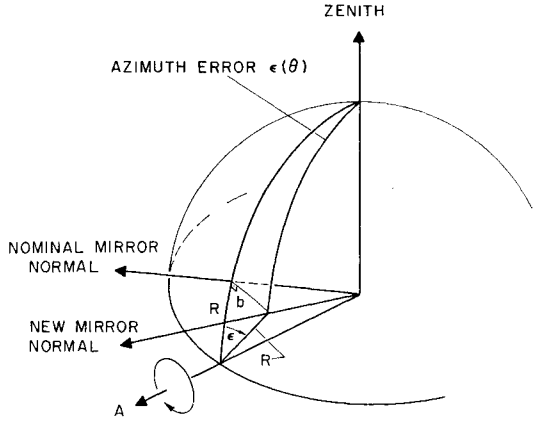

Fig. 12 Movement of mirror normal for nonhorizontal azimuth transfer.

Appendix: Effects of Errors in Level, and Required Positional Accuracy

Tolerable Error in Level

If the instrument is misleveled by rotating about a horizontal axis A by an amount ϵ (see Fig. 11), then the azimuth of the mirror will change by an amount $\epsilon(\theta)$, where

$$\tan\epsilon(\theta) = (1 - \cos\epsilon)/(\cot R + \cos\epsilon \tan R) \qquad \text{(A1)}$$

For small angles

$$\epsilon(\theta) = (\epsilon^2/2) \sin R \cos R \leq \epsilon^2/4 \qquad \text{(A2)}$$

Thus, if we want $\epsilon(\theta) < 0.2$ arcsec, we can allow misleveling up to 7 arcmin. Therefore, no special knowledge of level is required, nor does the instrument have to be precisely leveled prior to operation.

Nonhorizontal Azimuth Transfer

If nominal azimuth transfer is inclined by angle R (Fig. 12) to the horizontal, then level errors are more critical. From the figure, we can again compute

$$\tan\epsilon(\theta) = \sin\epsilon \tan R/(1 - \sin^2\epsilon \sin^2 R)^{1/2} \qquad \text{(A3)}$$

which becomes $\epsilon(\theta) = \epsilon \cdot R$ if both ϵ and R are small. If, for example, a nominally horizontal transfer is desired, then for $\epsilon(\theta) < 0.2$ arcsec, both ϵ and R should be less than 3.3 arcmin. If, on the other hand, transfer is nominally at $R = 10°$, then we must have $\epsilon < 1.2$ arcsec, which is a reasonably stringent requirement. One can see, therefore, a rapid increase in stability and level problems as the transfer angle deviates appreciably from horizontal.

Azimuth Correction due to Level Error

Although small errors in level will not significantly affect the actual azimuth of the mirror (as seen earlier), the computed value based on star transits will be erroneous because the computed optical axis direction does not coincide with the zenith. Correcting the computed azimuth θ' (Fig. 13) for this error involves transferring (λ', ϕ') into (λ, ϕ), wherein the angle A remains constant, thereby causing a change in azimuth to θ. It can be shown from Fig. 13 that

$$\tan\Delta\theta/2 = (\cos\phi + \sin\phi \tan\Delta\phi/2) \tan\Delta\lambda/2 \qquad \text{(A4)}$$

where ϕ = latitude and $\Delta\phi$ and $\Delta\lambda$ are the differences in latitude and longitude, respectively, of the known and computed site positions. For small angles this reduces to

$$\Delta\theta = \Delta\lambda \cos\phi \qquad \text{(A5)}$$

accurate to 0.27 arcsec as long as $\Delta\phi$ and $\Delta\lambda$ are each less than 7 arcmin. Thus, level deviations (<7 arcmin) in latitude can be ignored and the correction for longitude level effects is quite simple.

Required Positional Accuracy

From the preceding paragraph it can be seen that to the azimuth uncertainty derived from individual star transits will be added errors caused by lack of positional knowledge in applying the correction there derived. From Eq. (A5), the variance $\epsilon^2(\Delta\theta)$ in the correction $\Delta\theta$ is

$$\epsilon^2(\Delta\theta) = \cos^2\phi\ \epsilon^2(\Delta\lambda) + (\Delta\lambda)^2 \sin^2\phi\epsilon^2(\phi)$$

Let us take the second term first. As said above, $\Delta\lambda$ has a maximum value of 7 arcmin and $\phi \sim 45°$. For the second term to contribute less than 0.2 arcsec to $\Delta\theta$, $\epsilon(\phi)$ cannot exceed

$$0.2 \text{ arcsec}/(7 \text{ arcmin} \times 0.707) = 2.3 \text{ arcmin}$$

Thus, latitude of the site need only be known to about two miles.

The first term is due to longitude uncertainties. Again, for $\phi \sim 45°$ and $\epsilon(\Delta\theta) < 0.2$ arcsec, $\epsilon(\Delta\lambda)$ cannot exceed $0.2/0.707 = 0.28$ arcsec. Thus, longitude must be known to better than 30 ft, and corresponding clock errors must be kept below a similar number of milliseconds.

References

[1] Berg, R. T., "Measurement of the Astronomic Azimuth of a Mirror Normal," Test Pad Stability Symposium No. 4, May 15–16, 1963, Honeywell, Inc., Minn.

[2] Pavlov, N. N., "The Photoelectric Registration of Star Transits," *Publications of the Central Observatory at Pulkova*, Ser. II, Vol. LIX, Leningrad, 1946.

[3] Liang, T.-Y., "Determination of Time, Longitudes, Latitudes and Azimuths by the Photoelectric Method," *Geodesy and Aerophotography*, No. 1, 1963, pp. 32–38.

[4] Moreau, R. L., "Photoelectric Observations in Geodetic Astronomy," *Canadian Surveyor*, Vol. 20, No. 4, 1966, pp. 282–291.

[5] Abby, D. G., "Development of an Electro-Optical Theodolite," XI Pan American Consultation on Cartography, 1969, Pan American Institute of Geography and History, Washington, D.C.

[6] Carroll, J. E., "A New Instrument for the Determination of Astronomic Position," *Surveying and Mapping*, Sept. 1969, Vol. XXIX, No. 3, pp. 447–461.

[7] *Smithsonian Astrophysical Observatory Star Catalog*, Smithsonian Publication 4652, Supt. of Documents, U.S. Government Printing Office, Washington, D.C. 20402, 1966.

[8] Berg, R., private communication, July 1969, Honeywell, Inc., Minneapolis, Minn.

NOVEMBER 1970 J. SPACECRAFT VOL. 7, NO. 11

Reaction-Boom Attitude Control Systems

W. W. Hooker,* I. P. Leliakov,† M. G. Lyons,‡ and G. Margulies§
Lockheed Missiles & Space Co., Sunnyvale, Calif.

Active gravity-gradient stabilization systems are shown to permit significant improvement in the stabilization and maneuvering capability of Earth-pointing satellites compared to more conventional momentum storage and mass expulsion techniques. The proposed configuration consists of the payload body and a properly arranged array of gimballed "reaction booms." The appropriate boom gimbals are torqued on the basis of payload attitude and gimbal sensor data. Qualitatively, the system may be viewed as a hybrid that derives rapid momentum transfer and payload maneuvering capability from active torquing between the component parts of the satellite, while obtaining the necessary momentum dumping from gravity-gradient torques acting on the over-all configuration. The number, geometry, and hinging of the booms is dependent on the specific control or maneuvering requirements; therefore, three distinct system types are proposed. Procedures for selecting control laws are developed on the basis of simplified dynamic models, and the expected system performance is verified through simulation of both linearized and full nonlinear system models. The observed payload response resembles that of a fast reaction-wheel system. Low-frequency, gravity-gradient modes are effectively decoupled from payload motion and boom oscillations are satisfactorily constrained even for large-angle payload steering maneuvers.

Nomenclature

c_i = damping coefficient
$\bar{E}_i$ = orbiting reference axes, i = 1,2,3
$\bar{e}_i$ = payload body axes, i = 1,2,3
f,g $\equiv 4\Omega^2$ and $3\Omega^2$, respectively
θ_i = main body roll, pitch, yaw angles with respect to the orbiting reference axes, i = 1,2,3
α_i,β_i = relative roll and pitch boom gimbal angles for the i^{th} boom, i = 1,2,3,4
H_i = momentum of reaction wheel aligned with $\bar{e}_i$, i = 1,2,3
I = payload moments of inertia
J = reduced moments of inertia of one boom (about axis normal to boom and relative to composite system CM)
k = spring coefficient
T_i' = torque on reaction wheel parallel to $\bar{e}_i$, i = 1,2,3
$T_{\alpha i}',T_{\beta i}'$ = torques on the α and β gimbals of the i^{th} boom,¶ i = 1,2,3,4
Ω = mean orbit rate
ω_n = natural frequency
ζ = damping ratio

Received September 11, 1969; revision received August 12, 1970.

* Research Scientist, Mathematics & Operations Research Laboratory.
† Staff Engineer, Guidance & Flight Mechanics Department.
‡ Senior Research Engineer, Attitude Stability & Control Systems Department. Member AIAA.
§ Senior Staff Scientist, Mathematics & Operations Research Laboratory.

¶ For configurations A and B, i = 1.